



## Research paper

## Fabrication of Micro Glass Spherical Resonator by Chemical Foaming Process (CFP)

M. Kookhaee, A. Khooshehmehri, A. Eslami Majd\*

Faculty of Electrical and Computer, Malek-Ashtar University of Technology, Tehran, Iran.

### Article Info

#### Article History:

Received 05 January 2022

Reviewed 10 March 2022

Revised 26 April 2022

Accepted 07 May 2022

#### Keywords:

Hemispherical resonator gyroscope

The etched cavity in the silicon substrate

Anodic bonding

Glass blowing

Height to radius ratio of the shell

\*Corresponding Author's Email

Address: [a\\_eslamimajd@mut-es.ac.ir](mailto:a_eslamimajd@mut-es.ac.ir)

### Abstract

**Background and Objectives:** The Hemispherical Resonator Gyroscope (HRG) is an inertial sensor which is a good choice for space missions and inertial navigation due to their low noise, low energy consumption, long life, and excellent accuracy and sensitivity. It consists of three main parts: the shell, the excitation and detection system, and the control circuits. In recent years, with using MEMS technology in the construction of HRG, vibrating shells with low volume and low price are made.

**Methods:** The hemispherical shell is the main part and the beating heart of hemispherical resonator gyroscopes and is responsible for sensing. An optimized shell is required to implement the excitation and detection system and operate the gyroscope properly. In this research, the structure of a spherical shell with an environmental base that does not need to release the shell from its environment for its excitation and detection system is selected and the relationships governing this type of shell to improve the parameters of the glass blowing method will be investigated. Also, all sub-processes of this type method of fabrication to optimize the glass-blown spherical shell are implemented.

**Results:** The process of making spherical shell by glass blowing using the chemical foaming process is used to obtain shells with height to radius ratio greater than 1, and finally, a glass shell with an etched cavity with a radius of 562  $\mu\text{m}$  and depth of 524  $\mu\text{m}$  created by the CNC process, with height to radius ratio of approximately 1.8 has been achieved. In this method, using direct transfer of calcium carbonate to the etched cavity, before anodic bonding, the glass shell volume has been increased from 0.602 nL to 1.04 nL.

**Conclusion:** The result is that to achieve a glass shell with a height to radius ratio of more than 1, in addition to improving the fabrication process, it is necessary to transfer the solid foaming agent to the etched cavity. Finally, in the fabrication of the glass-blown spherical shell, we have used the chemical foaming process (CFP) to obtain shells with a height to radius ratio greater than 1.

This work is distributed under the CC BY license (<http://creativecommons.org/licenses/by/4.0/>)



### Introduction

Coriolis vibration gyroscopes are sensors in which the angle of rotation or angular velocity is measured using the Coriolis force applied to the vibrating mass [1]. One of the types of Coriolis vibration gyroscopes is the vibrating shell

gyroscopes that vibrate with a hemispherical resonator or so-called "wine glass" [2], [3].

Hemispherical resonator gyroscopes (HRG) are considered a suitable choice for space missions and inertial navigation due to their low noise, low energy

consumption, long life, and excellent accuracy and sensitivity [4]. These types of gyroscopes can also be made microelectromechanically [5].

The structure of a hemispherical resonator gyroscope consists of three main parts: the shell, the excitation, and detection system, and the control system. The resonator shell is the main part and the beating heart of these gyroscopes and is responsible for sensing. The resonator shell needs a perfectly symmetrical structure for proper operation to show desirable characteristics in terms of equilibrium, natural frequency difference, vibration-induced deformation, and damping [6].

Due to the diversity of the structure of resonator shells, different methods are used to make the shell, which can be mainly referred to as two methods of silicon-based bulk and surface micromachining and surface tension processes [7]. In the construction of the shell by micromachining process using several stages of photolithography and etching, the resonator shell is created in the substrate [8].

The fabrication of the shell by surface tension processes is also based on the surface tension force at the melting point of the materials and is done in the two methods of blow torching [9] and glass blowing [10].

In 2014, Taheri-Tehrani *et al.* Reported the construction of a hemispherical shell with a diameter of 1 mm, depth of 250  $\mu\text{m}$ , and thick of 1  $\mu\text{m}$  by micromachining process. In this method, the diamond shell is fabricated by the chemical vapor deposition (CVD) process in cavities created by wet and isotropic etch [11].

In 2015, Khalil Najafi *et al.* Created shells using the blow torching process. In this fabrication method, the shell with its solid stem is separated from the mold and finally released using a type of wax and chemical mechanical polishing (CMP) [12]. In 2018, Dingbang Xiao *et al.* Also examined the process of making a shell by blowtorching and releasing it with a femtosecond laser to improve the cutting quality of the side walls [13], [14].

In 2015, Senkal *et al.* Reported the fabrication of a micro-fused silica shell using the glass blowing process [15].

In 2015, Senkal investigated the fabrication of pyrex shells by the glass blowing process. In the mentioned thesis, DRIE was used to etch cylindrical cavities with a central post to a depth of 250  $\mu\text{m}$  on a 1mm silicon wafer. In this reference, to evaluate the structure of the hemispherical resonator shell, characteristics such as structure symmetry, shell surface roughness, and material composition before and after glass blowing have been analyzed [10].

In 2015, AM Shkel *et al.* Reported the fabrication of a spherical shell by glass blowing and surrounding electrodes, in which a pyrex micro-spherical resonator with a radius of 500  $\mu\text{m}$  was made by glass blowing

process and surrounded by four electrodes. In the process of fabricating this shell, cylindrical cavities with a radius of 265 nm and a depth of 800  $\mu\text{m}$  are created by dry etching (DRIE) on a 1 mm silicon wafer [16].

AM Shkel *et al.* In 2011 and Binzhen Zhang *et al.* In 2016 proposed a method for glass-blown spherical shell fabrication with three-dimensional metal electrodes created at the same time as the shell [17], [18].

In 2018, Jianbing Xie *et al.* Used a method of transferring the solid foaming agent ( $\text{CaCO}_3$ ) using a precipitation reaction to etched cavities by the DRIE process before anodic bonding to achieve larger sphericity. The tallest spherical glass shell, created by an etched cavity with a radius of 250  $\mu\text{m}$  and a depth of 800  $\mu\text{m}$ , has a height to radius ratio of 1.58 [19].

Jintang Shang *et al.* In 2011 and 2015 also used  $\text{TiH}_2$  foaming agents to fabricate glass bubbles [20], [21].

An optimized shell is required to use the shell as a sensor and to measure the amount of input rotation to the resonator. In fact, to implement the excitation and detection system, one must first obtain a shell with the desired structural features to design and then implement the excitation and detection system according to its geometry. In this research, we have selected to implement a glass-blown spherical shell with an environmental base that does not need to release the shell from its surroundings for its excitation and detection system. The sub-processes of the glass blowing method include etching cavities, anodic banding, thinning and polishing, and blowing. We used the CNC process to create etched cavities in a silicon substrate. Using this method in creating cavities with great depth takes less time. After implementing all the sub-processes of this type of method of fabrication and improving their parameters, the glass shell with a height to radius ratio of more than 1, was still not obtained. To achieve a glass shell with a desired height to radius ratio ( $>1$ ), in addition to improving the fabrication process, we used the direct transfer of the solid foaming agent (calcium carbonate) to the etched cavity before the anodic bonding process.

Finally, we have achieved a spherical shell with a height to radius ratio of approximately 1.8 by creating an etched cavity with a radius of 562  $\mu\text{m}$  and a depth of 524  $\mu\text{m}$  using the CNC process and direct transfer of calcium carbonate to the etched cavity. Although our cavity radius was greater, and our cavity depth was less than the values used in similar articles, we were able to achieve a glass shell very close to the sphere by the chemical foaming process.

### Governing Relationships the Spherical Shell with Peripheral Base

To improve the glass blowing process, it is necessary to study the governing relationships of the spherical shell. The geometrical parameters of the glass-blown spherical

shell are shown in Fig. 1 where  $R_0$  is the radius of the etched cavity,  $h$  is the depth of the etched cavity,  $R_g$  is the radius of the spherical shell and  $h_1$  is the height of the spherical shell.

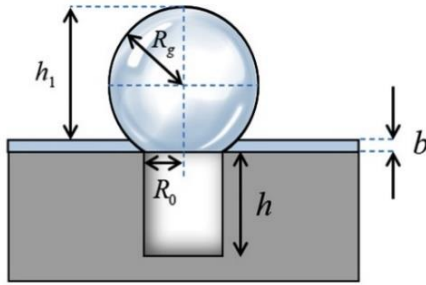


Fig. 1: Display of geometric parameters of a spherical shell with peripheral base.

The impact of gravity and the viscous force of the softened glass are neglected in the height model, and the thickness of the glass shell is considered to be uniform; hence, the volume of expanded gas confined obeys the ideal gas law.

Using the geometric parameters shown in Fig. 1, the volume of the etched cavity can be obtained from (1) [19]:

$$V_E = \pi R_0^2 h \quad (1)$$

According to Fig. 1, where  $R_0$  is the radius of the etched cavity,  $h$  is the depth of the etched cavity. The volume of the glass shell can also be obtained using (2) [19]:

$$V_g = \left(\frac{T_f}{T_b} - 1\right)V_E \quad (2)$$

where  $V_g$  represents the volume of the glass shell,  $V_E$  represents the volume of the etched cylindrical cavity,  $T_f$  represents the furnace's heating temperature, and  $T_b$  represents the anodic bonding temperature. Thus, considering the volume of the etched cavity and the volume of the glass shell, the height of the glass shell as a function of the furnace temperature, bonding temperature, depth, and radius of the etched cavity can be obtained using (3) [19]:

$$h_1 = \frac{\left[\left(3V_g + \sqrt{R_0^6 \pi^2 + 9V_g^2}\right)\pi^2\right]^{\frac{2}{3}} - R_0^2 \pi^2}{\pi \left[\left(3V_g + \sqrt{R_0^6 \pi^2 + 9V_g^2}\right)\pi^2\right]^{\frac{1}{3}}} \quad (3)$$

The mathematical equation describing the relationship between the height of the glass shell ( $h_1$ ) and the radius of the glass shell ( $R_g$ ) is (4) [19]:

$$R_g = \frac{R_0^2 + h_1^2}{2h_1} \quad (4)$$

### Fabrication of the Glass-Blown Spherical Shell

The steps of fabricating a glass-blown spherical shell have five main sub-processes; include etching cavities,

transfer the solid foaming agent to the etched cavity, anodic banding, thinning and polishing, and blowing. The schematic of this type of fabrication is shown in Fig. 2.

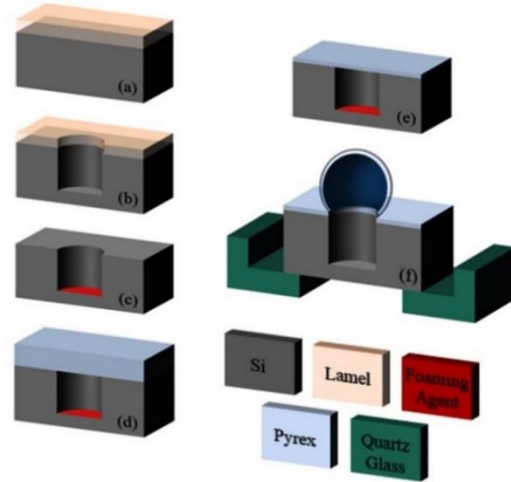


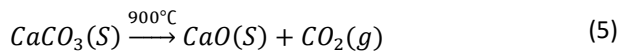
Fig. 2: Schematic of the process of fabricating a glass-blown spherical shell by chemical foaming process. (a) Paste the lamel to silicon and preparing it for the CNC process, (b) Creating a cylindrical cavity in a p-type silicon substrate using the CNC process, (c) Direct transfer of the solid foaming agent ( $\text{CaCO}_3$ ) into the etched cavity, (d) Anodic bonding of pyrex layer to silicon substrate, (e) Decreasing the thickness of the pyrex layer to  $200 \mu\text{m}$  using the thinning and polishing process, (f) Putting the sample on a quartz base and transfer it to a furnace to form a glass shell.

The young's modulus of the substrate has a greater effect on the quality factor (Q) of the resonator than its density, in other words, the substrate with a higher young's modulus leads to less energy loss. Silicon substrate with a higher young's modulus is a better choice than fused silica substrate [22]. Silicon substrate consists of two common types n and p [23], for the reason that the p-type silicon substrate has a better performance in the anodic bonding process than the n-type substrate, it is better to use this type of substrate [24].

In the cavities etching process, first, a p-type silicon substrate with a thickness of  $740 \mu\text{m}$  is selected and a cavity with a radius and depth of  $550 \mu\text{m}$  is created on it using the CNC process. In creating a cavity with a CNC machine, by measures such as changing the tool movement program, reducing the tool speed, changing the tool, and pasting the lamel on the silicon, it is possible to improve the lip and the dimensions of the cavity and bring it closer to the ideal (Fig. 2 (a), (b)). The crystalline orientation of the silicon substrate does not affect the creation of a cavity using CNC [30].

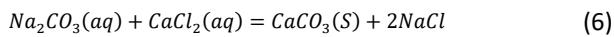
Then, to increase the height to radius ratio of the glass shell, the solid foaming agent is transferred into the etched cavity in the silicon (Fig. 2 (c)). Here, for the process of adding the foaming agent, calcium carbonate ( $\text{CaCO}_3$ ) with the thermal decomposition temperature of  $825 \text{ }^\circ\text{C}$  is used as a foaming agent, which its chemical

decomposition is in the furnace heating temperature in (5) [25]:



This material's thermal decomposition temperature is lower than that of the furnace (~900 °C) but greater than that of anodic bonding (~400 °C), thus it fits the requirements of the following procedure.

Calcium carbonate (CaCO<sub>3</sub>) can be transferred into the etched cavity inside the silicon substrate in two ways, using direct transfer and the precipitation reaction of Na<sub>2</sub>CO<sub>3</sub> solution and CaCl<sub>2</sub> solution. The chemical equation (6) is used to place the foaming agent into the etched cavity using a precipitation reaction:



In the precipitation reaction method, two syringe pumps and two microliter syringes with a needle with an outer diameter of 190 μm are used to inject solutions into the cavity. The outer diameter of the syringe needle is smaller than the diameter of the etched cavity. The quantity of calcium carbonate in the etched cavity may be adjusted by varying the injected volume and concentration of the two reaction solutions. The sample is put on a hot plate after the micron-injection procedure, and the determined amount of calcium carbonate (CaCO<sub>3</sub>) is left in the cavity [19].

In this paper, the direct transfer is used to transfer the solid foaming agent into the etched cavity in silicon. Directly transferring the solid foaming agent is very difficult. There are two primary causes for this difficulty: one, solid calcium carbonate (particularly powders) would cause difficult-to-remove bonding surface contamination, and the second, CaCO<sub>3</sub> is insoluble in most solvents [19]. In the direct transfer of the solid foaming agent, calcium carbonate powder is first mixed with DI water to form a suspension. Using a microliter syringe with a needle with an outer diameter of 300 μm, the suspension is injected into the cavity. After DI water evaporates, calcium carbonate powder settles to the bottom of the cavity.

The cleanliness of the silicon surface is very important at this step because the powder particles remaining on the surface will not cause proper bonding of silicon and pyrex and will lead to problems in subsequent processes [24]. In this process, the amount of gas emitted by the foaming agent may be regulated by adjusting the number of moles of calcium carbonate (CaCO<sub>3</sub>), which is equivalent to the number of moles of CO<sub>2</sub>.

Next, the silicon wafer with the cavity is anodically bonded to a pyrex layer, at a temperature of 400 °C and a voltage of 1500 V, and the air and the solid foaming agent are trapped inside the etched cavity in the silicon (Fig. 2 (d)). In the anodic bonding process, the roughness of the two surfaces that are placed on top of each other is so

important that two samples with a surface roughness of more than 50 nm in this process, at the higher the applied temperature and voltage, are not connected.

Bond strength is a critical element in the anodic bonding process since it is related to bond quality and dependability. A good bond is created when the bond strength is high. As the bonding temperature increases, the bond strength increases [26]. In the fabrication of a spherical shell by glass blowing, reducing the bonding temperature increases the air pressure trapped inside the etched cavity and improves the height to radius ratio of the shell. This decrease in bonding temperature may create unbonded points near the cavity, which will cause problems such as reduced air pressure inside the cavity, breaking pyrex during thinning, and asymmetry of the shell.

The use of mechanical tests, such as pressure, pull, shear, or bending tests to evaluate the anodic bonding process is not desirable because it destroys the specimen and makes it impossible to continue the fabrication process [24]. In this paper, an optical microscope, which is a non-destructive method, has been used to evaluate the anodic bonding process. In this method, using the color difference, the bonded spots and the unbonded spots are determined. A visual evaluation to observe unbonded spots is shown in Fig. 3.

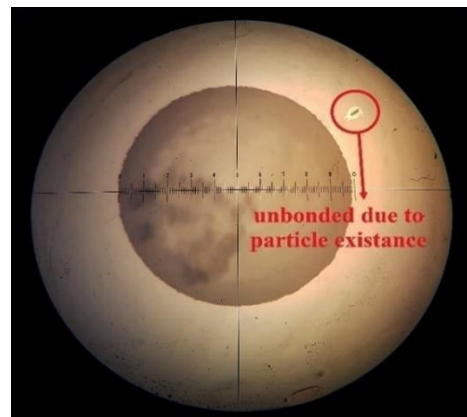


Fig. 3: Examination of unbonded spots using color differences using an optical microscope.

The thickness of the pyrex layer bonded to the silicon substrate with an etched cavity should be something around a few hundred micrometers [27], [28]. In this paper, a thickness of 200 μm is considered as the desired thickness, which can be used to Achieve this desired thickness using the thinning and polishing process (Fig. 2 (e)).

In this step of the fabrication process, in order to form the glass shell, the bonded wafer with the pyrex layer facing upwards is placed onto a quartz glass stencil and then both together are transferred into the quartz tube furnace (Fig. 2 (f)). The type of furnace used in this step

depends on the softening point of the bonded pyrex (820 °C). To prevent shock to the bonded wafer, it is transferred to the center of the furnace in 3.5 minutes.

While glass can be shaped at a broad range of temperatures, empirical tests show that if the furnace temperature is less than 800 °C, the glass spheres will take a long time to form. Also, because of the poor viscosity at higher temperatures, the spheres tend to break if the furnace temperature is higher than 950 °C. Therefore, the best temperature range for the furnace is between 850 °C and 900 °C [29].

By placing the bonded wafer at a temperature higher than the softening point of pyrex (870 °C) in a furnace, the trapped air in the cavity and the gas produced by the calcium carbonate expand and increase the pressure inside the cavity. However, this increase in pressure occurs via the uniform surface pressure distribution before driving the high-temperature molten glass membrane to reshape into a hollow shell. As the pyrex layer softens and the gas is released by the foaming agent at the furnace temperature, the thin pyrex layer on top of the cavity that has been etched in silicon substrate becomes a spherical glass shell. The surface tensile force in this method causes high symmetry and minimal roughness on the surface of the spherical shell [18].

After 20-60 seconds, the formed shells will be removed quickly to cool down in the air in order to avoid the collapse of the shells. The heating time should be chosen carefully because if the heating time is very long, the glass shell would deform even break. On the other hand, if the heating time is not long enough, the glass would not have enough time to become soften and blown into hemisphere shape [19].

**Experimental Characteristics**

In the governing relationships of the spherical shell, the radius of the etched cavity ( $R_0$ ), the depth of the etched cavity ( $h$ ), the temperature at which the etched cavity was bonded to a glass wafer ( $T_b$ ), and the heating temperature in the furnace ( $T_f$ ) are considered as inputs and the height of the spherical shell ( $h_1$ ) and the radius of the spherical shell ( $R_g$ ) is calculated as output.

The hollow glass shell that is more similar to a sphere could provide more favorable properties of the hemispherical resonator gyroscope. The larger the height to radius ratio of the glass shell, it is closer to being spherical and therefore more desirable.

The advantages of the high ratio of height to a radius of the glass shell can be referred to reducing four-node wineglass resonant frequency, which is useful for the excitation and detection of the HRG, and larger surface area for adjustment higher aspect surrounding capacitive electrodes, which can increase the sensitivity of HRG [19]. Therefore, two parameters of the height to radius ratio of the glass shell ( $h_1/R_g$ ) and the height to diameter ratio of

the glass shell ( $h_1/2R_g$ ) are also considered as output parameters. The effect of changing the radius of the etched cavity on the height to radius ratio of the shell is shown in Fig. 4.

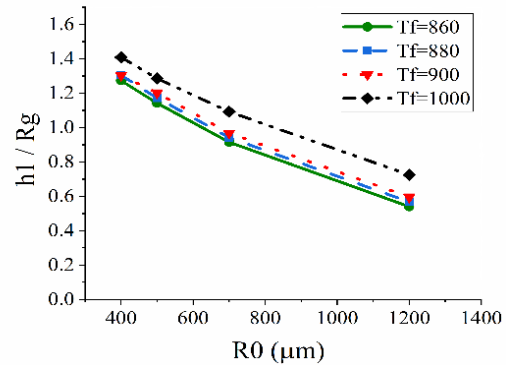


Fig. 4: The effect of changing the radius of the etched cavity on the height to radius ratio.

In the diagram in Fig. 4, the depth of the etched cavity (600  $\mu\text{m}$ ) and the anodic bonding temperature (400 °C) is considered constant, and the radius of the etched cavity and the heating temperature in the furnace has been changed. As can be seen in Fig. 4, as the radius of the etched cavity increases, the height to radius ratio of the glass shell decreases, and as the heating temperature in the furnace increases, the height to radius ratio of the glass shell increases. Also, the effect of changing the depth of the etched cavity on the height to radius ratio of the shell is shown in Fig. 5.

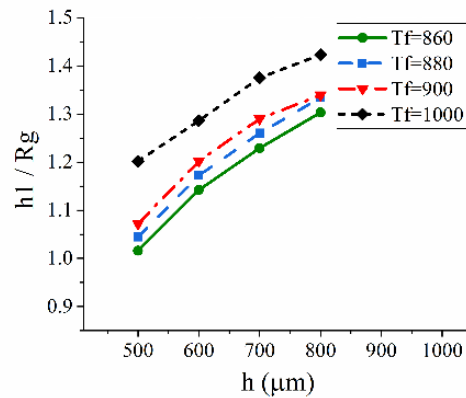


Fig. 5: The effect of changing the depth of the etched cavity on the height to radius ratio.

In the diagram in Fig. 5, the radius of the etched cavity (500  $\mu\text{m}$ ) and the anodic bonding temperature (400 °C) are considered constant, and the depth of the etched cavity and the heating temperature in the furnace has been changed. As can be seen in Fig. 5, as the depth of the etched cavity and the heating temperature in the furnace increase, the height to radius ratio of the glass shell increases. The effect of the temperature of anodic bonding change on the height to radius ratio of the shell is shown in Fig. 6.

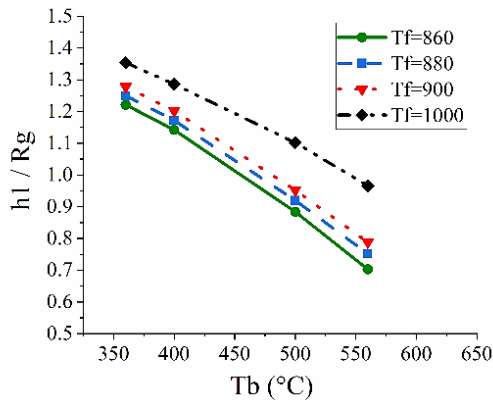


Fig. 6: The effect of the temperature of anodic bonding change on the height to radius ratio.

In the diagram in Fig. 6, the radius (500 μm) and depth (600 μm) of the etched cavity are considered constant, and the anodic bonding temperature and the heating temperature in the furnace have been changed. As can be seen in Fig. 6, as the anodic bonding temperature increases, the height to radius ratio of the glass shell decreases, and as the heating temperature in the furnace increases, the height to radius ratio of the glass shell increases. The effect of the heating temperature in the furnace change on the height to radius ratio of the shell is shown in Fig. 7.

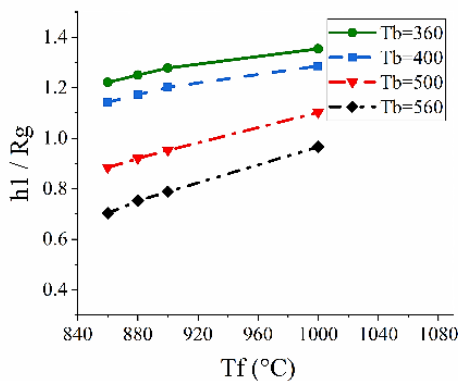


Fig. 7: The effect of the temperature in the furnace change on the height to radius ratio.

In the diagram in Fig. 7, Similar to the diagram in Fig. 6, the radius and depth of the etched cavity are considered constant, and the heating temperature in the furnace and the anodic bonding temperature have been changed. As it is known, in the diagram of Fig. 7, with increasing the heating temperature in the furnace, the height to radius ratio of the glass shell increases, and with increasing the anodic bonding temperature, the height to radius ratio of the glass shell decreases.

This result is obtained from the analysis of the above diagrams that to achieve the height to radius ratio of the glass shell of more than 1, the radius of the etched cavity and the anodic bonding temperature should be reduced

and the depth of the etched cavity and the heating temperature in the furnace should be increased.

The depth and radius of the etched cavity, the thickness of the pyrex layer, the anodic bonding temperature, the temperature at which the glassblowing was executed, and even the cooling process of the softened glass shell all play an important role in the final shape of the glass shell [10], [19].

By performing the sub-processes of fabrication include etching cavities, anodic banding, thinning and polishing, and blowing, the glass shell is formed. It is difficult to obtain a glass shell with a height to radius ratio greater than 1 with these sub-processes. To obtain the glass shell with a height to radius ratio of more than 1, methods such as reducing the radius of the etched cavity and the anodic bonding temperature and increasing the depth of the etched cavity and the heating temperature in the furnace have been performed. These changes applied have been effective in increasing the height to radius ratio of the glass shell, but the result is far from a spherical shell, and the volume of the glass shell is still under restrictions from the process parameters. In addition, applying these changes has been faced challenges. For example, a thick silicon substrate is needed to increase the depth of the etched cavity (800-1000 μm). In this paper, to increase the depth of the etched cavity, a layer of pyrex with a thickness of 2 mm is anodically bonded to the double side polished silicon substrate from the back to provide the depth of the cavity to be increased. Then, to create an etched cavity using the CNC process, the sample is pasted on the lam in such a way that the silicon is facing up, and a lamel is glued on it to improve the lip. The image and schematic of this prepared sample are shown in Fig. 8.

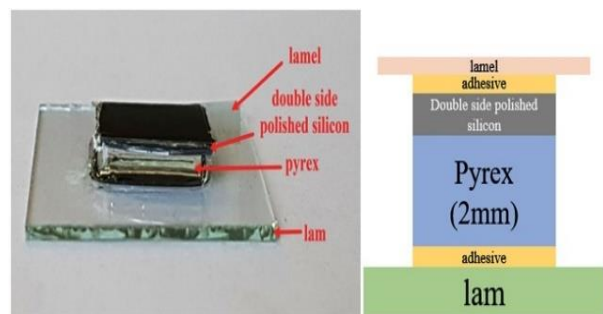


Fig. 8: Anodic bonding the pyrex wafer to the double side polished silicon substrate to increase the depth of the etched cavity.

Increasing the thickness of the sample causes prolongation of time in the fabrication process and increases the cost. In addition, it affects subsequent processes and makes the anodic bonding and dicing processes difficult [19], [29]. One of the problems with increasing the thickness is the need to apply a very high voltage (2600 V) to perform the anodic bonding process

of the upper pyrex layer at low temperatures (400 °C). Applying excessive voltage during the anodic bonding process increases the likelihood of the sample sparking and breaking. Demonstration sample 1 is shown in Fig. 9.

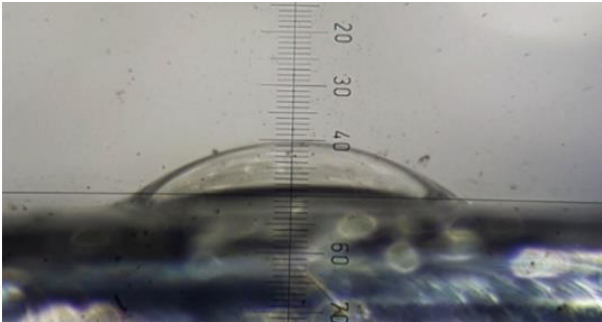


Fig. 9: Demonstration glass shell created by optimizing the four sub-processes of etching cavity, anodic banding, pyrex thinning and polishing, and blowing.

In Fig. 9, the glass shell is created by optimizing the four sub-processes of etching cavity, anodic banding, pyrex thinning and polishing, and blowing.

As shown in this figure, the glass shell created is spaced from the spherical shell and has a height to radius ratio of below 1.

**Results and Discussion**

In this work, to achieve a glass shell with a height to radius ratio of more than 1, in addition to improving the fabrication sub-processes, transferring the foaming agent to the etched cavity has also been used.

First, two cavities with the same conditions and dimensions are created using a CNC process inside a silicon substrate and some foaming agent (CaCO<sub>3</sub>) is transferred into one of these cavities.

Fig. 10 (a) shows a spherical shell blown via an etched

cavity in silicon substrate without a foaming agent and Fig. 10 (b) shows a spherical shell blown via an etched cavity in a silicon substrate with a quantified foaming agent.

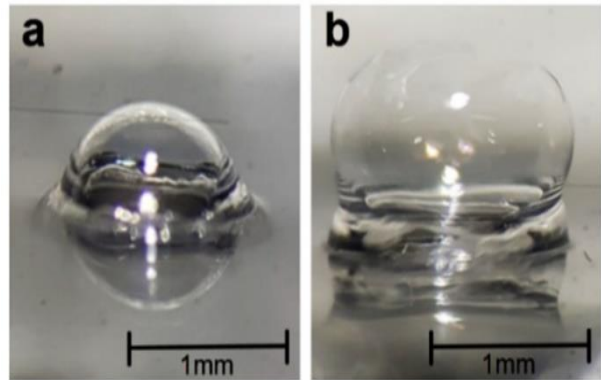
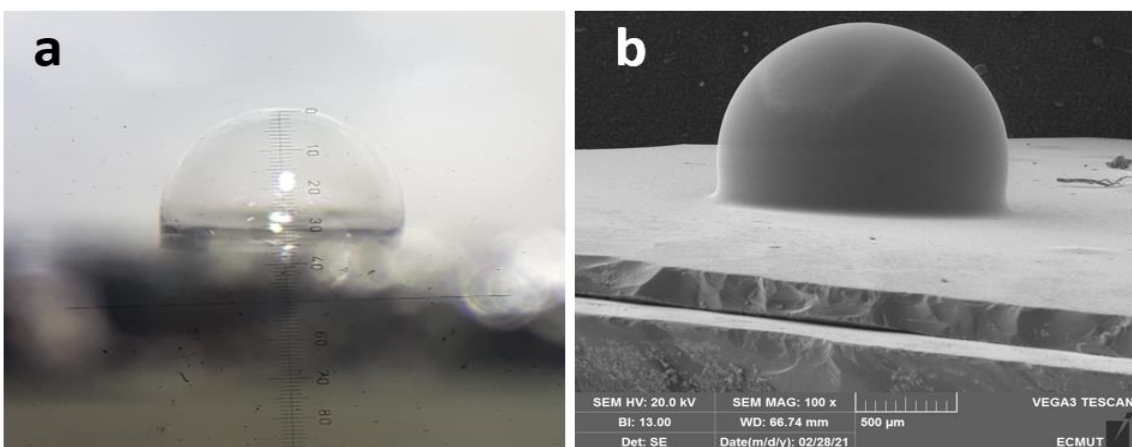


Fig. 10: (a) Spherical shell blew via an etched cavity in silicon substrate without a foaming agent, (b) Spherical shell blew via an etched cavity in a silicon substrate with a quantified foaming agent.

As shown in Fig. 10, the height to radius ratio of the glass shell that in its fabrication process used the foaming agent is greatly improved compared to the glass shell that there is only air in the etched cavity.

The height to radius ratio of the hemispherical shell resonators (HSRs), With the addition of foaming agent in the etched cavity to a depth of 200 μm may approach (even exceed) the shell has been blown by the etched cavity to a depth of 800 μm without no addition foaming agent [19].

Fig. 11 shows the optical microscope and scanning electron microscope (SEM) images of spherical shells created by the chemical foaming process (samples 2 and 3).



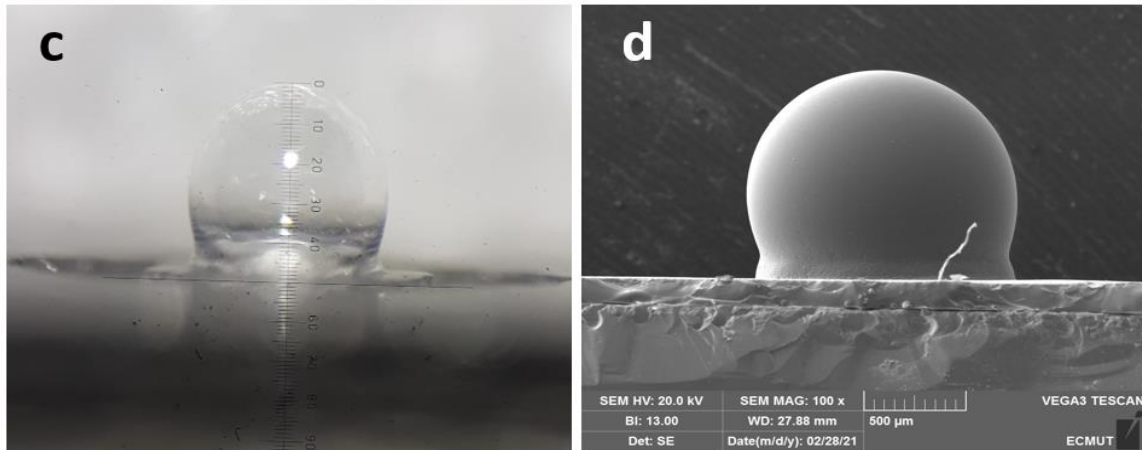


Fig. 11: Optical microscope and scanning electron microscope (SEM) images of spherical shells created by the chemical foaming process. (a, b) Sample 2. (c, d) Sample 3.

The experimental parameters and the experimental results of the samples in Fig. 11 are reported in Table 1. According to the governing relationships of the spherical shell, if the foaming agent not used in the fabrication of the glass shell of sample 2, ideally it should have reached a height of 472  $\mu\text{m}$  and a radius of 550  $\mu\text{m}$ , in which case the height to radius ratio of the shell is below 1. Sample 2, using the foaming agent ( $\text{CaCO}_3$ ), the approximate height and radius of the glass shell 931  $\mu\text{m}$  and 655  $\mu\text{m}$  were achieved, respectively, and the height to radius ratio

of the shell reached 1.42.

Also, if the foaming agent not used in the fabrication of the glass shell of sample 3, ideally it should have reached a height and radius of 553  $\mu\text{m}$  and 560  $\mu\text{m}$ , respectively, in which case the height to radius ratio of the shell is less than 1. Sample 3, using the foaming agent ( $\text{CaCO}_3$ ), has reached the approximate height and radius of the glass shell of 1129  $\mu\text{m}$  and 637  $\mu\text{m}$ , respectively. As can be seen, the glass shell of sample 3 is very close to the sphere and its height to radius ratio is approximately 1.8.

Table 1: The experimental parameters and the experimental results of the glass shell samples

Sample	Input							Output					
	$R_0$ ( $\mu\text{m}$ )	$h$ ( $\mu\text{m}$ )	$e$ ( $\mu\text{m}$ )	$b$ ( $\mu\text{m}$ )	$T_b$ ( $^\circ\text{C}$ )	$T_f$ ( $^\circ\text{C}$ )	$t$ (min)	$h_1$ (predicted) ( $\mu\text{m}$ )	$h_1$ ( $\mu\text{m}$ )	$R_g$ (predicted) (mm)	$R_g$ ( $\mu\text{m}$ )	$\frac{h_1}{R_g}$ (predicted)	$\frac{h_1}{R_g}$
	the radius of the etched cavity	the depth of the etched cavity	edge of the etched cavity	the thickness of the glass wafer	the anodic banding temperature	the heating temperature in the furnace	the heating time in the furnace	the predicted height of the glass shell	the height of the glass shell	the predicted radius of the glass shell	the radius of the glass shell	the predicted height to radius ratio of the glass shell	the height to radius ratio of the glass shell
1	587.5	796	20	200	400	870	1.5	732	250	0.60	-	1.216	-
2	550	422	10	175	400	870	0.45	472	930.80	0.55	654.78	0.858	1.42
3	562.5	524	10	125	400	870	0.33	553	1128.71	0.56	636.25	0.987	1.77

### Conclusion

In this study, to optimize the glass-blown spherical shell, all the sub-processes of this type of fabrication method, including etching cavity, anodic banding, pyrex

thinning and polishing, and blowing, have been carefully investigated and implemented in practice. In spherical shell optimization, the result is that to achieve a glass shell with a height to radius ratio of more than 1, in addition to

improving the fabrication sub-processes, it is also necessary to transfer the foaming agent to the etched cavity. Finally, using the chemical foaming process (CFP) and direct transfer of calcium carbonate to the etched cavity by the CNC process with a radius of 562  $\mu\text{m}$  and a depth of 524  $\mu\text{m}$ , before the anodic bonding process, a glass shell with a height to radius ratio of approximately 1.8 has been obtained.

### Author Contributions

All the authors participated in the conceptualization, implementation and M. Kookhae wrote the manuscript.

### Funding

The authors received no special funding for this effort.

### Acknowledgment

The authors would like to acknowledge the Faculty of Electrical & Computer Engineering, Malek Ashtar University of Technology, and the Microelectronic laboratory, for their support and contribution to this study.

### Conflict of Interest

The authors declare no potential conflict of interest regarding the publication of this work. In addition, the ethical issues including plagiarism, informed consent, misconduct, data fabrication and, or falsification, double publication and, or submission, and redundancy have been completely witnessed by the authors.

### Abbreviations

<i>MEMS</i>	Micro-Electro-Mechanical Systems
<i>HRG</i>	Hemispherical Resonator Gyroscope
<i>DRIE</i>	Deep Reactive Ion Etching
<i>CVD</i>	Chemical Vapor Deposition
<i>CNC</i>	Computer Numerical Control
<i>SEM</i>	Scanning Electron Microscopy
<i>CMP</i>	Chemical Mechanical Polishing

### References

- [1] J. Lee, S. Yun, J. Rhim, "Design and verification of a digital controller for a 2-Piece hemispherical resonator gyroscope," *Sensors*, 16(4): 555, 2016.
- [2] A. M. Shkel, "Type I and type II micromachined vibratory gyroscopes," in *Proc. IEEE/ION PLANS 2006*: 586-593, 2006.
- [3] Z. Xu, G. Yi, M. Er, C. Huang, "Effect of uneven electrostatic forces on the dynamic characteristics of capacitive hemispherical resonator gyroscopes," *Sensors*, 19(6): 1291, 2019.
- [4] A. A. Trusov, M. R. Phillips, G. H. Mccammon, D. M. Rozelle, A. D. Meyer, "Continuously self-calibrating CVG system using hemispherical resonator gyroscopes," in *Proc. 2015 IEEE International Symposium on Inertial Sensors and Systems (ISISS)*: 1-4, 2015.
- [5] A. Heidari, M. L. Chan, H. A. Yang, G. Jaramillo, P. Taheri-Tehrani, P. Fonda, H. Najar, K. Yamazaki, L. Lin, D. A. Horsley, "Hemispherical wineglass resonators fabricated from the microcrystalline diamond," *J. Micromech. Microeng.*, 23(12): 125016, 2013.
- [6] Z. Xu, G. Yi, H. Fang, Y. Cao, L. Hu, G. Zhang, "Influence of elasticity modulus on the natural frequency in hemispherical resonator," in *Proc. 2019 IEEE DGON Inertial Sensors and Systems (ISS)*: 1-11, 2019.
- [7] B. Luo, M. A. Zhang, C. Lu, J. Shang, "Wafer-level fabrication of silicon-in-glass electrodes for electrostatic transduction," in *Proc. 2016 IEEE 66th Electronic Components and Technology Conference (ECTC)*: 1278-1283, 2016.
- [8] J. J. Bernstein, M. G. Bancu, J. M. Bauer, E. H. Cook, P. Kumar, E. Newton, T. Nyinjee, G. E. Perlin, J. A. Ricker, W. A. Teynor, M. S. Weinberg, "High Q diamond hemispherical resonators: fabrication and energy loss mechanisms," *J. Micromech. Microeng.*, 25(8): 085006, 2015.
- [9] J. Cho, J. Yan, J. A. Gregory, H. Eberhart, R. L. Peterson, K. Najafi, "High-Q fused silica birdbath and hemispherical 3-D resonators made by blow torch molding," in *Proc. 2013 IEEE 26th International Conference on Micro Electro Mechanical Systems (MEMS)*: 177-180, 2013.
- [10] D. Senkal, "Micro-glassblowing Paradigm for Realization of Rate Integrating Gyroscopes," PhD Thesis University of California, Irvine, 2015.
- [11] P. Taheri-Tehrani, T. Su, A. Heidari, G. Jaramillo, C. Yang, S. Akhbari, H. Najar, S. Nitzan, D. Saito, L. Lin, D.A. Horsley, "Micro-scale diamond hemispherical resonator gyroscope," in *Proc. Hilton Head Workshop*: 289-292, 2014.
- [12] J. Y. Cho, K. Najafi, "A high-q all-fused silica solid-stem wineglass hemispherical resonator formed using micro blow torching and welding," in *Proc. 2015 28th IEEE International Conference on Micro Electro Mechanical Systems (MEMS)*: 821-824, 2015.
- [13] W. Li, Z. Hou, Y. Shi, K. Lu, X. Xi, Y. Wu, X. Wu, D. Xiao, "Application of micro-blowtorching process with whirling platform for enhancing frequency symmetry of microshell structure," *J. Micromech. Microeng.*, 28(11): 115004, 2018.
- [14] Y. Shi, X. Xi, Y. Wu, W. Li, K. Lu, Z. Hou, X. Wu, D. Xiao, "Wafer-level fabrication process for micro hemispherical resonators," in *Proc. 2019 IEEE 20th International Conference on Solid-State Sensors, Actuators and Microsystems & Eurosensors XXXIII (TRANSDUCERS & EUROSensors XXXIII)*: 1670-1673, 2019.
- [15] D. Senkal, M. J. Ahamed, M. H. Asadian Ardakani, S. Askari, A. M. Shkel, "Demonstration of 1 million q-factor on microglassblown wineglass resonators with out-of-plane electrostatic transduction," *J. Microelectromech. Syst.*, 24(1): 29-37, 2015.
- [16] J. Giner, A. M. Shkel, "The concept of "collapsed electrodes" for glassblown spherical resonators demonstrating 200: 1 aspect ratio gap definition," in *Proc. 2015 IEEE International Symposium on Inertial Sensors and Systems (ISISS)*: 1-4, 2015.
- [17] I. P. Prikhodko, S. A. Zotov, A. A. Trusov, A. M. Shkel, "Microscale glass-blown three-dimensional spherical shell resonators," *J. Microelectromech. Syst.*, 20(3): 691-701, 2011.
- [18] R. Wang, B. Bai, H. Feng, Z. Ren, H. Cao, C. Xue, B. Zhang, J. Liu, "Design and fabrication of micro hemispheric shell resonator with annular electrodes," *Sensors*, 16(12): 1991, 2016.
- [19] J. Xie, L. Chen, H. Xie, J. Zhou, G. Liu, "The application of chemical foaming method in the fabrication of micro glass hemisphere resonator," *Micromachines*, 9(2): 42, 2018.
- [20] J. Shang, B. Chen, W. Lin, C.P. Wong, D. Zhang, C. Xu, J. Liu, Q. A. Huang, "Preparation of wafer-level glass cavities by a low-cost chemical foaming process (CFP)," *Lab on a Chip*, 11(8): 1532-1540, 2011.
- [21] B. Luo, J. Shang, Y. Zhang, "Hemippherical wineglass shells fabricated by a Chemical foaming process," in *Proc. 2015 IEEE 16th International Conference on Electronic Packaging Technology (ICEPT)*: 951-954, 2015.
- [22] A. Darvishian, B. Shiari, J. Y. Cho, T. Nagourney, K. Najafi, "Anchor loss in hemispherical shell resonators" *J. Microelectromech. Syst.*, 26(1): 51-66, 2017.

- [23] G. S. May, S. M. Sze, *Fundamentals of Semiconductor Fabrication*, USA: Hoboken, John Wiley & Sons, 2004.
- [24] A. C. Lapadatu, H. Jakobsen, *Handbook of Silicon Based MEMS Materials and Technologies (Second Edition)*, Chapter 30, Anodic Bonding (pp. 599-610) Elsevier BV, 2015.
- [25] R. Barker, "The reversibility of the reaction  $\text{CaCO}_3 \rightleftharpoons \text{CaO} + \text{CO}_2$ " *J. Appl. Chem. Biotechnol.*, 23(10): 733-742, 1973.
- [26] J. Wei, H. Xie, M. L. Nai, C. K. Wong, L. C. Lee, "Low temperature wafer anodic bonding" *J. Micromech. Microeng.*, 13(2): 217-222, 2003.
- [27] C. Zhang, A. Cocking, E. Freeman, Z. Liu, S. Tadigadapa, "On-Chip glass microspherical shell whispering gallery mode resonators," *Sci. Rep.*, 7(1): 14965, 2017.
- [28] J. Giner, L. Valdevit, A. M. Shkel, "Glass-blown pyrex resonator with compensating Ti coating for reduction of TCF," in *Proc. 2014 IEEE International Symposium on Inertial Sensors and Systems (ISISS)*: 1-4, 2014.
- [29] E. J. Eklund, A. M. Shkel, "Glass blowing on a wafer level," *J. Microelectromech. Syst.*, 16(2): 232-239, 2007.
- [30] A. Khooshehmehri, A. Eslami Majd, S. A. Hosseini, "Design and fabrication of hemispherical shell resonator by glass blowing method," *J. Electr. Comput. Eng. Innovations*, 10(1): 37-46, 2022.

## Biographies



**Maryam Kookhaee** was born in Tehran in Iran, 1993. She received the B.Sc. degree in Bioelectrical Engineering from Sahand University of Technology, Tabriz, Iran, in 2016. Also, she received the M.Sc. degree in Electrical Engineering from Malek-Ashtar University of Technology in 2021. Her research interests include Coriolis Gyros, MEMS, and semiconductor field effect devices.

- Email: [maryam\\_kookhaee@mut.ac.ir](mailto:maryam_kookhaee@mut.ac.ir)
- ORCID: [0000-0002-1991-6954](https://orcid.org/0000-0002-1991-6954)
- Web of Science Researcher ID: NA
- Scopus Author ID: NA
- Homepage: NA



**Aylar Khooshehmehri** received the B.Sc. degree in Electrical Engineering from K. N. Toosi University of Technology, Tehran, Iran, in 2007. Also, she received the M.Sc. and Ph.D. degree in Electrical Engineering from Malek-Ashtar University of Technology in 2011 and 2018, respectively. Her research interests include superconducting amplifying and detector devices, MEMS, and semiconductor field effect devices.

- Email: [khooshehmehri@mut.ac.ir](mailto:khooshehmehri@mut.ac.ir)
- ORCID: NA
- Web of Science Researcher ID: NA
- Scopus Author ID: NA
- Homepage: NA



**Abdollah Eslami Majd** was born in Hamadan, Iran, on March 23, 1976. He received the B.E. degree in applied physics from bu-ali Sina University, Hamadan, Iran in 1998. He received M.E. degree in atomic and molecular physics from Amir kabir University of Technology Tehran Polytechnic, Tehran, Iran in 2001. He received the Ph.D. Degree in photonics from laser and plasma Institute of Shahid Beheshti University, Tehran, Iran in 2011.

Since joining electrical engineering and electronic department of Malek Ashtar University of Technology in 2012, he has engaged in research and development of starry light in the satellite camera, laser induced breakdown spectroscopy (LIBS) and hemispherical resonator gyroscope (HRG). He is co-author of more than 30 publications. Dr. Eslami is a member of Optics and Photonics Society of Iran and Physics Society of Iran.

- Email: [a\\_eslamimajd@mut-es.ac.ir](mailto:a_eslamimajd@mut-es.ac.ir)
- ORCID: [0000-0002-7538-3160](https://orcid.org/0000-0002-7538-3160)
- Web of Science Researcher ID: NA
- Scopus Author ID: NA
- Homepage: NA

### How to cite this paper:

M. Kookhaee, A. Khooshehmehri, A. Eslami Majd, "Fabrication of micro glass spherical resonator by Chemical Foaming Process (CFP)," *J. Electr. Comput. Eng. Innovations*, 11(1): 65-74, 2023.

DOI: [10.22061/JECEI.2022.8737.549](https://doi.org/10.22061/JECEI.2022.8737.549)

URL: [https://jecei.sru.ac.ir/article\\_1719.html](https://jecei.sru.ac.ir/article_1719.html)

